DOI: 10.15480/882.9324

Eighth International Symposium on Marine Propulsors
smp'24, Berlin, Germany, March 2024

# Upgraded MMG-Methodology to Capture Gate-Rudder Performance Aspects

**Norbert Bulten**

Wärtsilä Propulsion, Drunen, The Netherlands

## ABSTRACT

The Gate-Rudder concept is one of the ideas which is investigated in the EU-project CHEK to reduce the vessel emissions. The research in this project is based on full-scale CFD simulations of a bulker vessel. The conventional scope has been extended with vessel-drift and rudder-steering actions, which are expected to occur when the CHEK bulker is equipped with wind-assisted propulsion. The CFD results for vessel drift and rudder angles have revealed interesting findings when the rudder performance is compared to conventional rudders. To cover a larger range of vessel operating conditions a dynamic system simulation model is created, based on the CFD dataset. This model gives the vessel operating condition (RPM, vessel drift and rudder angle) for given vessel speed and external force. The published MMG method has been adapted to implement the specific behavior of the Gate-Rudder. With the adjusted method comparisons can be made between the reference case and the Gate-Rudder concept. It has been found that the performance of the Gate-Rudder is especially good in case of some disturbances like drift and rudder angle, which is regarded to be typical for CII performance. Therefore, the use of the straight-sailing, calm water condition as representative vessel operating condition must be reconsidered.

## Keywords

Gate-Rudder, propulsion, CFD, CHEK, CII

## 1 INTRODUCTION

In the last couple of years, several vessels have been equipped with the Gate-Rudder™ technology. First vessels are sailing in the coastal area of Japan, and more recently a vessel has been retrofitted in Turkey as part of the GATERS EU-project. Unanimous feedback from all vessels was a clearly observed fuel saving in actual operation and improved maneuverability (Sasaki et al 2019). The Gate-Rudder (GR) should thus not only be evaluated on its merits to control the vessel course keeping and maneuvering as a rudder, but also as an energy saving device in combination with the propeller (Mizzi et al 2022, Zammit Munro et al 2023). More detailed information about the Gate-Rudder concept will be given in section 2.

Given the coming regulations regarding CII, the focus in ship design and building will move from design-for-sea trial to design-for-operation. The significant savings of the GR as found in operation are to be understood properly for future applications.

So far, the more conventional research methods have been used: towing tank experiments and Computational Fluid Dynamics (CFD) simulations. Running the vessel in straight sailing direction in calm water has not revealed the origin of the significant fuel savings. However, some typical aspects of the GR have been found in both the experiments and the simulations. When applying a rather subtle change of the two Gate-Rudder blade angles in a symmetrical way (toe-in or toe-out), the forces on the two rudder-blades change significantly. Moreover, the propeller loading changes a couple of percent. This indicates that the local flow phenomena around the rudder leading edge are important and there is a clear interaction with the propeller loading. The local flow phenomena near the rudder leading edge will be influenced by the vessel motions, vessel drift and wave patterns among others. Having that in mind, one can raise the question whether the standard straight-sailing calm-water approach excludes some of the benefits of the GR. To get better insights in the aspects of disturbed inflow phenomena the scope of CFD simulations has been extended to study the impact of vessel drift, turning rate and rudder angle.

This work has been executed as part of the EU-project CHEK. In this project a new concept design for a bulker vessel is studied, with the target to reduce the emissions as much as possible. This is to be accomplished by applying wind-assisted-ship-propulsion (WASP), air-lubrication, anti-fouling and a large, slow running propeller with a Gate-Rudder. Section 3 will give some more details on the CHEK project bulker variant.

Coupling of the forces and moments from the WASP with the hydrodynamics of the hull, the propeller and the rudder is one of the challenges in the CHEK-project. The possible operating conditions, when harvesting the wind, will result in a large number of potential operating conditions. It is therefore proposed to develop a dynamic vessel model based on a multi-parameter approach. The model is based on full-scale CFD simulations with pre-defined vessel drift and rudder steering actions. A description of the numerical method is given in section 4. The comparison of a conventional rudder and a Gate-Rudder revealed interesting results for both the vessel-drift variation as well as the rudder-angle variation. The CFD results are translated into a set of multi-parameter response surfaces. These data-sets are used in a similar way as the well-known MMG-model (Yasukawa & Yoshimura, 2015) in a vessel maneuvering model. The dynamic simulation model and its currently implemented features is described in section 5. Some reflections on the proposed changes of the vessel maneuvering model are discussed in section 6. The conclusions of the ongoing research are stated in Section 7, as well as the outlook for the work which still needs to be done.

## 2 GATE-RUDDER TECHNOLOGY

The concept of the Gate-Rudder will be explained in more detail below. Two typical aspects of operation are brought to the attention as well: toe-in impact and propeller load reduction.

### 2.1 Gate-Rudder Concept

The Gate-Rudder concept is developed some years ago in Japan (Sasaki et al 2021). This rudder concept is not only used for the maneuvering and course-keeping of the vessel, but also acting as a kind of duct. This interacting with the propeller results in reduction of propeller loading. As a result, the Gate-Rudder can be regarded as an Energy Saving Device. Comparison of the fuel consumption of various sailing vessels with their sister vessels with conventional rudders have shown clear reductions for the Gate-Rudder equipped vessels. In the GATERS project a vessel has been retrofitted with Gate-Rudder and there the differences in power and fuel consumption before and aft of the conversion were significant. (Sasaki, N., Atlar, M., 2023). Figure 1 shows a photo of one of the vessels equipped with the Gate-Rudder.

### 2.2 Toe-in & Toe-out Operation

The two rudder blades, as shown in Figure 1, are operated based on a single rudder-steering command. This aspect is thus similar to conventional rudders. However, due to the symmetrical execution of the two Gate-Rudder blades, the blades can be rotated, whilst balancing the sway forces. This is called Toe-in & Toe-out operation (when looking from above towards the bow, moving the leading edges inward means toe-in, as shown in Figure 5). This aspect is an addition compared to a conventional rudder.

A series of full-scale CFD simulations has been made to get an impression of the impact of this toe-in/toe-out angle on the rudder forces. At the same time the propeller-loading has been varied to study the impact as well. Increased propeller loading results in a larger axial flow velocity through the propeller disk and possibly a change of the local angle of attack of the flow near the rudder leading edge. The results of the Toe-in/Toe-out CFD studies will be presented in section 4.2.

**Figure 1: Gate-Rudder Concept**

### 2.3 Course-keeping capability at reduced propeller load

The two blades of the gate-rudder are positioned alongside the propeller. The interaction between the propeller and rudder is therefore different when compared to conventional propeller-rudder configurations. This aspect is interesting when wind-assisted-ship-propulsion (WASP) is considered. The WASP will provide next to the surge-force a certain sway force, depending on the windspeed and direction (Elger et al 2020*)*. To handle the vessel course-keeping the rudder needs to steer to get the aerodynamic and hydrodynamic forces in equilibrium. The reduced propeller loading will reduce the effectiveness of the conventional rudder (based on MMG-logic) and therefore a larger rudder angle will be required when propeller loading goes down. Given the position of the Gate-Rudder blades, the dominant driving factor for the rudder forces is the vessel speed. It is therefore expected that the rudder-sway forces are less sensitive to propeller load reductions. The impact of propeller load reduction has been analyzed for a case of combined vessel drift and rudder angle. Results of the CFD simulations will be shown in section 4.5.

## 3 CHEK EU-PROJECT

The EU-project CHEK (Horizon2020 grant agreement No 955286) focusses on new, holistic vessel designs to reduce emissions drastically. In the project two vessel types are analyzed: bulker and cruise-vessel. In this paper a part of the work on the bulker vessel will be shown.

### 3.1 Bulker Vessel Emission Reduction Roadmap

To reach the challenging target of 50% energy saving various technologies are included in the new design. These comprise wind-assisted propulsion, air-lubrication system (ALS), ultrasonic anti-fouling and a gate-rudder. In addition, the driveline and engine configuration will be taken into account.

### 3.2 Bulker Vessel Hydrodynamic Redesign

Conventional bulker vessels are equipped with a fixed-pitch propeller (FPP) directly coupled to a 2-stroke engine, a layout that designers have applied to achieve a balanced performance in laden and ballast conditions. In the CHEK-project various technologies are to be combined on the vessel and therefore the operational envelope of the propeller will be larger. From hydrodynamic efficiency point of view a slow-running propeller is selected with largest possible diameter. To anticipate on the required operational flexibility, a controllable pitch propeller (CPP) is selected. The conventional rudder is replaced by a Gate-Rudder with same maneuvering characteristics. Figure 2 shows the two configurations. In CHEK project also the concept of a twin-screw bulker vessel is being investigated. However, the results of this work are not in scope of the current paper.

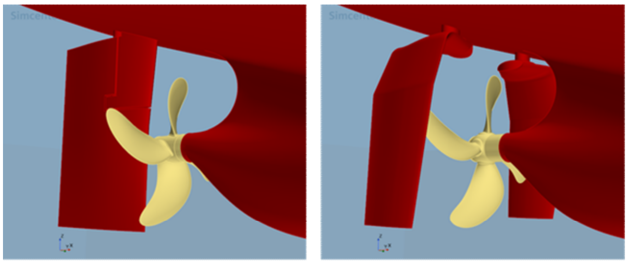

**Figure 2: CHEK Bulker Cases, left Reference Case with FPP and right Gate-Rudder with CPP**

### 3.3 Bulker Vessel Drive-line Layout

As mentioned in the previous section, the new concept is equipped with slow-rotating CP-propeller. To achieve the low propeller rotation-rate a gearbox is required to reduce the engine RPM. The need for a gearbox kind of opens the door to use 4-stroke engines, which run at higher speeds than 2-stroke engines. The actual CPP design RPM is actually lower compared to the FPP. This can be chosen freely based on the gearbox gear-ratio.

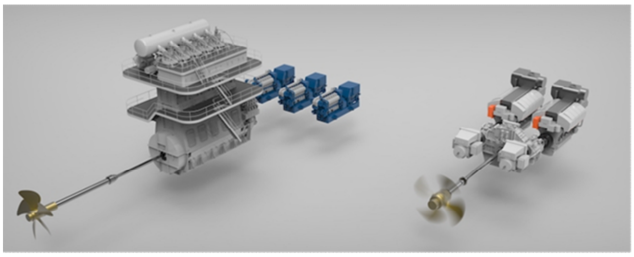

**Figure 3: CHEK Driveline Concepts, left Reference Case of Direct Coupled 2-Stroke Engine, right Twin-In-Single-Out Gearbox and Two 4-Stroke Engines**

The two driveline concepts are shown in Figure 3. To increase the operational flexibility even more, a twin-in-single-out (TISO) gearbox is selected. In case of low power demand, for example due to favorable wind-conditions, the gearbox can be driven by a single engine. In this way, the optimum loading of the engines can be selected over a large range, based on the variation of the used number of cylinders (single small engine, single large engine or both). Astern operation is handled by adjusting the propeller pitch, which does therefor not require a change of the engine rotation direction.

The main parameters of both configurations are shown in the table below.

**Table 1: Main Parameters of Reference and Gate-Rudder concept**

| | Reference | Gate-Rudder |
|---|---|---|
| **Propeller type** | FPP | CPP |
| **Diameter** | 7.3 | 7.4 |
| **Target RPM** | 76 | 60 |
| **Main engine** | 2-stroke | 4-stroke |
| **Gear-ratio** | 1.0 | 750/60 |

## 4 VESSEL CFD SIMULATIONS

In CHEK-project, the performance analysis of the Gate-Rudder concept is based on full-scale CFD simulations (a so-called 'in silico' approach) with Simcenter Star-CCM+. The background of the CFD approach will be briefly discussed in the following section. Some more background of the method has been presented by Sasaki et al (2021). The CFD model is set-up in such way that all parameter-variation studies could be executed with the same set-up. This gives a consistency regarding the numerical approach. In the subsequent sections the following parameter-studies will be presented: (a) toe-in angle, (b) vessel-drift angle, (c) rudder-steering angle, (d) propeller RPM combined with vessel drift and rudder angle.

### 4.1 Full-scale CFD Simulation Methodology

When considering all variations to be analyzed with CFD, it becomes clear that it will require an efficient workflow to process all cases. Therefore some simplifications in the CFD modelling have been made: the effects of free-surface and dynamic vessel motions, like dynamic sinkage and trim, are excluded. The free-surface boundary is set to symmetry-plane, which results in the known double-body approach. It is expected that the interaction between the flow along the rudder blades and the free-surface effects is limited, which allows this simplification of the numerical problem. The actual motion of the vessel is based on the rigid-body rotating arm motion, which allows for runs with vessel drift and turning rates in the same numerical set-up. The rotating arm is set to a 100km radius to simulate the straight sailing condition. To capture the interaction effects between the propeller, the rudders and the hull, the actual 3D propeller geometry is included in the simulations, which means a solution approach based on transient sliding mesh. The final time-step has been set equal to $2^{\circ}$ propeller rotation.

The rotating-arm rigid body motion has actually zero-velocity inlet boundary conditions, which requires some special attention to the turbulence modelling. The conventional approach of defining a certain Turbulence Intensity level will not work with zero inlet velocity and therefore the concept of ambient turbulence has been applied in conjunction with the Realizable k-ε model. The values for k and ε are based on the vessel speed, a Turbulence Intensity (TI) level of 1% and a Turbulent Viscosity Ratio (TVR) of 50.

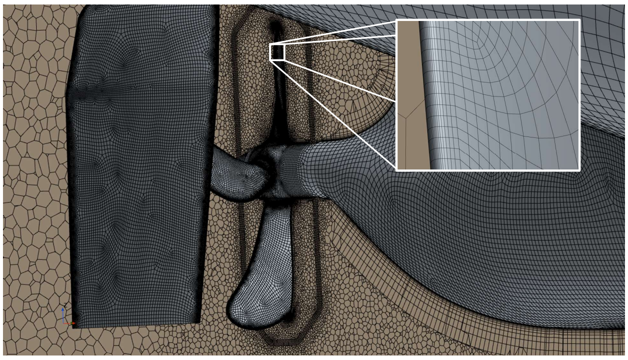

**Figure 4: Mesh of Vessel, Propeller and Rudder Based on Polyhedral Mesh and Anisotropic Advancing Layer Meshing**

Meshing of the domain is based on polyhedral cells in conjunction with Anisotropic Advancing Layer Meshing (AALM). With the anisotropic meshing the curvature of the propeller and rudder leading and trailing edges is captured well. The advancing layer meshing is used along the hull as well to capture the hull boundary layer development. This can be seen in Figure 4.

### 4.2 Toe-in Rudder Angles

A first parameter study has focused on the straight sailing condition with different propeller loadings and rudder toe-in angles. The concept of the Toe-in blade rotation is shown in Figure 5. Symmetrical movement of both rudder blades will not introduce a sway force, thus keeping the vessel going straight. The single blade rudder forces are monitored in the vessel coordinate system and translated to the rudder coordinate system depending on the rudder angle. The non-dimensional rudder lift $C_L$ is the equivalent of the rudder normal force $F_N$ as used in the MMG theory (Yasukawa & Yoshimura, 2015). The rudder drag Cd is perpendicular to the lift force. In case of the Gate-Rudder this force is actually a positively contributing thrust when a positive value is reported. In the MMG theory this force is referred to as a tangential rudder force and it is not being considered.

The range of toe-in rudder angles is rather small, only rotations in the range [$0^\circ$ - $4^\circ$] are considered. Variation in propeller RPM are limited to a few RPM as well, thought the range of power levels covers about 3000 to 6000 kW.

The rudder forces are defined in the rotating rudder coordinate system and made non-dimensional:

$$C_L = \frac{L}{\frac{1}{2}\rho \cdot A_R \cdot v_{ship}^2} \tag{1}$$

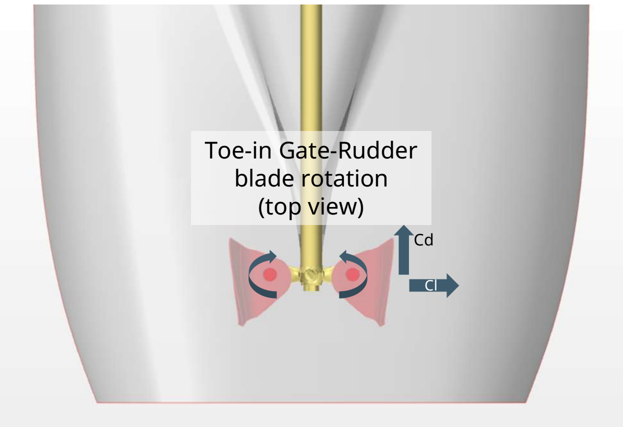

**Figure 5: Gate-Rudder Toe-In Blade Rotation Concept**

Figure 6 shows the rudder forces as function of the shaft power. The rudder lift force $C_L$ and the rudder thrust $C_D$ both increase significantly with a rudder deflection of $4^\circ$. The rudder thrust also increases with higher shaft power levels. This trend is opposite to conventional rudders, where the increased propeller loading results in increased velocities along the rudder, resulting in increased drag.

The results in Figure 6 show clear trends of the single blade rudder forces regarding the impact of power levels and rudder deflection. To get the impact on vessel operation the impact of both blades needs to be combined.

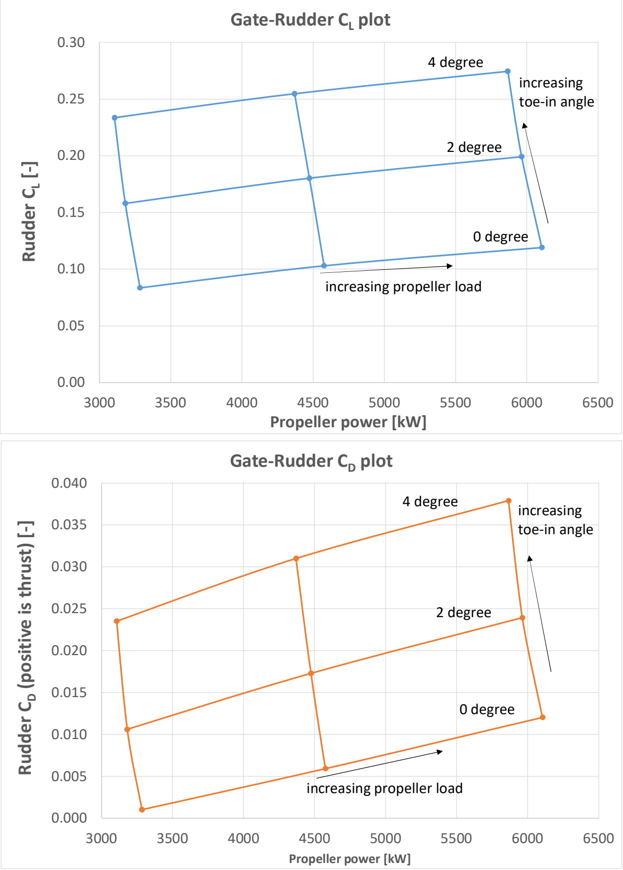

**Figure 6: Rudder Forces ($C_L$ & $C_D$) as Function of Shaft Power for Different Toe-In Angles**

The CFD simulations indicate that there is a subtle difference between the starboard and port rudder forces, which is attributed to the propeller rotation direction. It is therefore proposed to evaluate the combined performance of both rudder blades to eliminate this aspect of the propeller rotation.

Next to the interesting numerical results of the toe-in variation study it can be mentioned that similar results have been found in different model test measurement campaigns. These measurements were part of commercial projects and therefore more details can unfortunately not be disclosed.

### 4.3 Pre-defined Vessel Drift

The results from the toe-in study indicate that the local flow direction near the rudder leading edge could be important for the performance of the Gate-Rudder. Given the position of both blades outside of the hull boundary layer, it seems reasonable to assume that limited vessel drift could influence the behavior of the Gate-Rudder as well. The effect of vessel drift or yaw-motions is in general excluded from model testing in towing tanks and in CFD simulations.

A second motivation to look in more detail into the impact of vessel drift is related to the WASP, which is an important aspect in the CHEK project. When anticipating on the vessel course-keeping when using sails, a certain amount of vessel drift will occur.

As mentioned before, the numerical set-up with the rotating arm allows for implementation of vessel drift with a shift of the rotation center. The CFD simulations have been executed with drift to port and to starboard with constant propeller RPM and constant forward velocity. The rudder angle has been kept to 0 degree. More details about the impact of the propeller rotation direction will be given in the following subsection.

#### *4.3.1 Propeller loading during vessel-drift*

Due to the vessel drift the symmetrical wakefield of a single-screw propeller is disturbed. Figure 7 shows the inplane vectors just upstream of the propeller for drift to port and to starboard. The non-symmetrical pre-rotation of the flow leads either to an increase or a decrease of the propeller loading. The tangential component of the flow gives in fact an artificial change of the propeller RPM. The (artificial) change in RPM results in a different propeller thrust and torque, as shown in Figure 8. Since the pre-rotation is a result of the hull sailing with drift-angle, the effect is found for both the conventional reference rudder and the Gate-Rudder vessel.

The Kt-10Kq relation is shown in Figure 9 for both propellers. The RPM variation is shown with solid line and the drift-impact with the dotted line. The slow-running propeller design for the Gate-Rudder results in a larger Kt and 10Kq due to the difference in P/D-ratio. The impact of the load variations on the propeller thrust and torque are in line with the expected linear behavior.

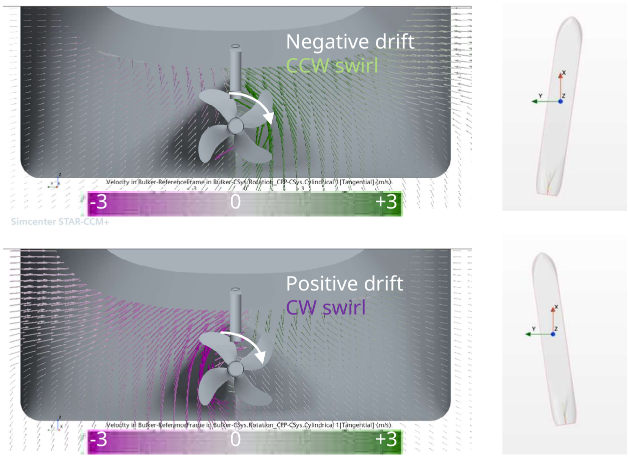

**Figure 7: Pre-Rotation for Negative (top) and Positive (bottom) Vessel Drift. Green Arrows Represent CCW Swirl, Pink Arrows represent CW-swirl.**

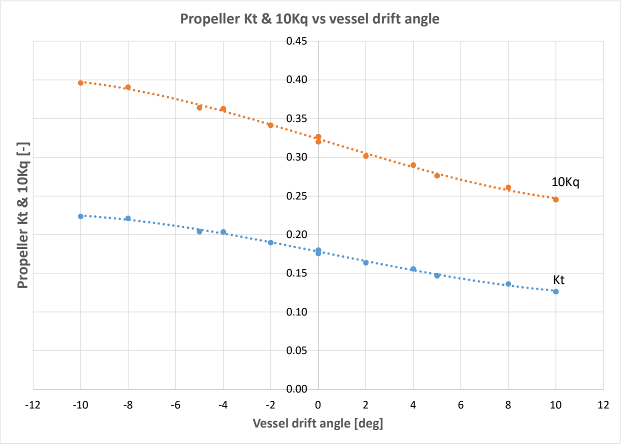

**Figure 8: Propeller Kt and 10Kq as Function of Vessel Drift Angle**

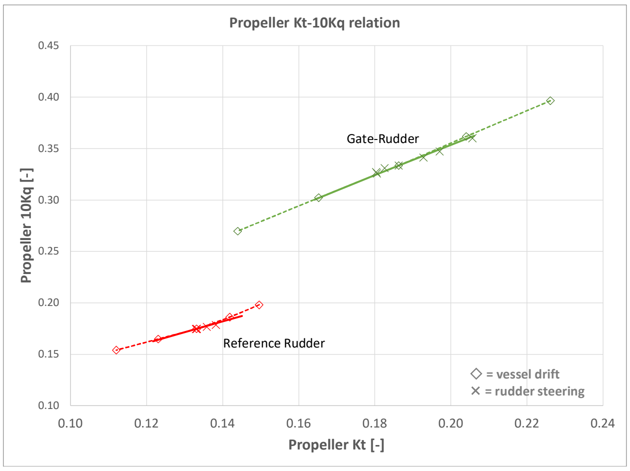

**Figure 9: Propeller Kt-10Kq Relation for Both Propellers Operating in Straight Sailing, with Vessel Drift and with Rudder Steering Action**

Many CFD researchers (Mizzi et al 2022, Zammit Munro et al 2023, Mucha et al 2023) make use of a Virtual Disk methodology to implement the propeller action. This approach obviously saves a lot of computation efforts. Nevertheless, it should be used with care in case of a non-symmetrical wake field. As long as the Virtual Disk methodology is based on the axial velocity distribution upstream, it will fail to take the effects of the pre-rotation into account. This applies to simulations including vessel drift and pre-swirl stator devices.

As discussed in more detail in the following section, even rudder steering action seems to have an impact on the propeller loading. This has also been shown by Aram & Mucha (2023).

### *4.3.2 Rudder thrust during vessel-drift*

As shown in the previous section, there is a clear interaction between the vessel drift and the propeller loading in the CFD simulations. It is acknowledged that the CFD runs are not based on force equilibrium but on constant vessel speed and propeller RPM.

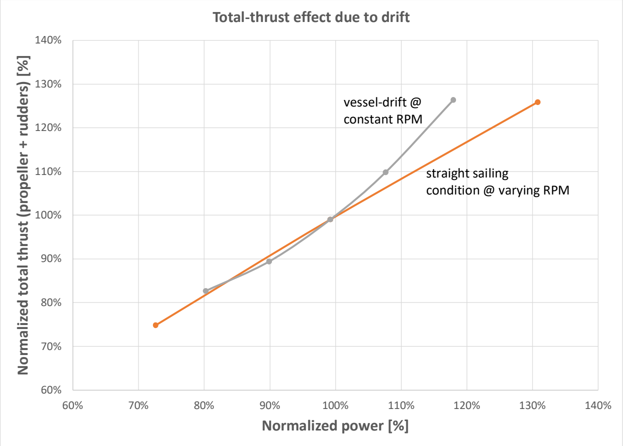

**Figure 10: Normalized Total Thrust as Function of Normalized Power for Straight Sailing and Vessel-Drift Conditions**

To isolate the different aspects, the impact of the propeller loading variation has to be compensated for. To evaluate the impact of the rudder thrust (or drag), the thrust of the propeller and rudder are combined. Figure 10 shows the comparison of the total-thrust versus power for the straight sailing case and the vessel-drift conditions. The straight line for normal sailing operation is based on a variation of propeller RPM.

To evaluate the additional thrust due to vessel-drift, the equivalent total thrust for that power level is determined. The difference between these two values is denoted as thrust bonus. The results for the thrust bonus calculation are shown in Figure 11 for both the reference rudder and the Gate-Rudder.

The trends found in this analysis are intriguing. The Gate-Rudder seems to perform significantly better compared to the reference rudder when the disturbances are larger. In the well-known condition of no drift, the differences are small. However, when the flow becomes more disturbed the gains for the Gate-Rudder are noticeable. A part of the gain is attributed to the change of the inflow angle to one of the two rudder blades. This will give additional thrust as has been observed in the toe-in study. The other blade will be in the shadow of the hull, which results in a lower performance, though the combined performance of both blades remains better.

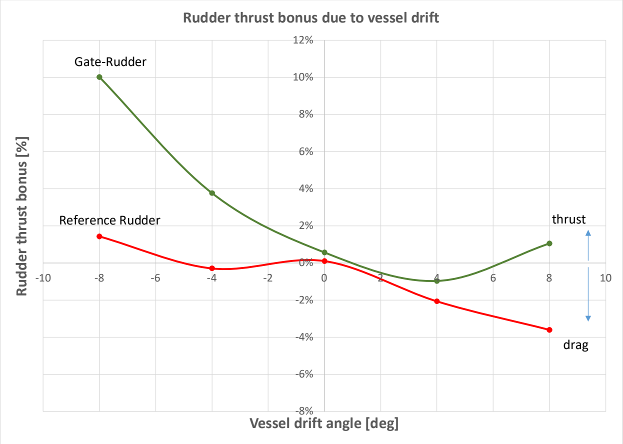

**Figure 11: Thrust Bonus as Function of Vessel Drift Angle**

## 4.4 Pre-defined Rudder Steering Angles

Another aspect of the rudder performance is the generated drag when steering. A series of CFD simulations has been made to determine the rudder steering performance whilst keeping the vessel at straight course. This could be regarded as the initial stage of a vessel maneuver. The CFD simulations are based on constant vessel speed and propeller RPM and zero drift.

To have a fair comparison between the two rudder concepts, the Gate-Rudder has been designed to generate similar sway-force and yaw-moment for the same rudder angles. The hull force sway coefficient comparison is shown in Figure 12, which proves that the design target has been met.

But, as shown in Figure 13, the rudder drag is significantly different when the reference rudder is compared to the Gate-Rudder. For small rudder angles, there is still a positive contribution of the Gate-Rudder blades to the vessel thrust.

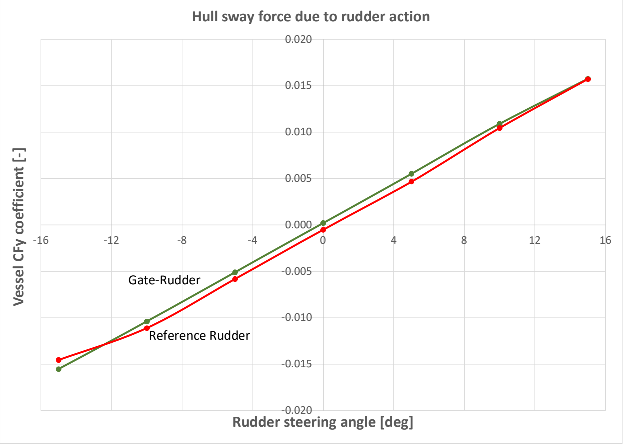

**Figure 12: Hull Sway Force Coefficient Comparison**

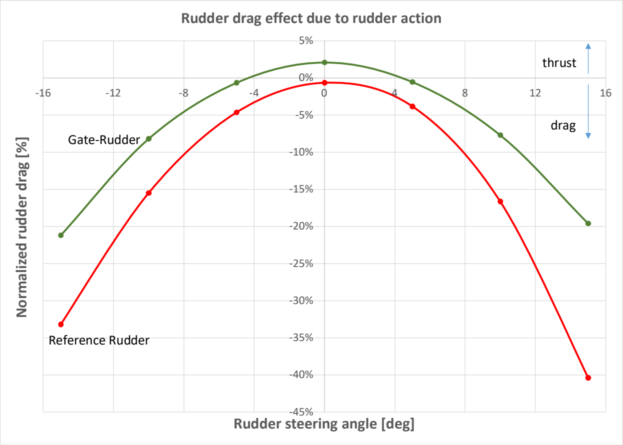

**Figure 13: Rudder Drag as Function of Rudder-Steering Action**

The chart as shown in Figure 9 also has a number of conditions included with the rudder steering angle variations. For the conventional rudder the steering action leads to a slightly increased propeller loading, probably due to larger blocking effect of the rudder. This trend is symmetrical with steering angle. When looking in more detail to the occurring flow phenomena of the Gate-Rudder, an asymmetry in the wake-field is found. Therefore, the propeller load variation has a similar effect as for the vessel drift. This aspect has been compensated for in Figure 13 to give a fair comparison based on equal power levels.

### 4.5 Impact of Propeller Load Reduction

In CHEK project the future bulker design is equipped with WASP systems. The benefits from wind-propulsion depend on the wind-speed and wind direction. Depending on the wind-direction, a certain amount of sway-force and yaw-moment from WASP will be generated. This needs to be compensated with the rudder. The actual WASP-vessel operating condition will be a combination of reduced propeller loading, vessel-drift and rudder-steering angle. In the previous two sections the impact on thrust (or surge) force has been discussed. For the WASP operation the aspect of sway and yaw equilibrium starts playing a role as well.

Based on the MMG theory (Yasukawa & Yoshimura, 2015), the sway force of the rudder is based on the rudder angle and the local inflow velocity. The longitudinal velocity $u_R$ is a function of the dimensions of the propeller and rudder and the actual propeller loading (based on J and Kt). Reduction of the propeller loading results in reduction of the rudder inflow velocity $U_R$. Since this velocity has a quadratic contribution to the rudder normal force $F_N$, the rudder sway force will decrease when reducing propeller loading.

Figure 14 shows the impact of rudder steering action at 5 degrees for the reference rudder and the Gate-Rudder as function of the propeller loading. The observed trend of reduced hull sway force with reduced propeller loading for the reference rudder is in line with expectation. The Gate-Rudder shows a different trend, with a small increase of hull sway force for reduced propeller loading. This effect is attributed to the constant vessel speed for all conditions, which seems to be the dominant velocity for the Gate-Rudder flow phenomena.

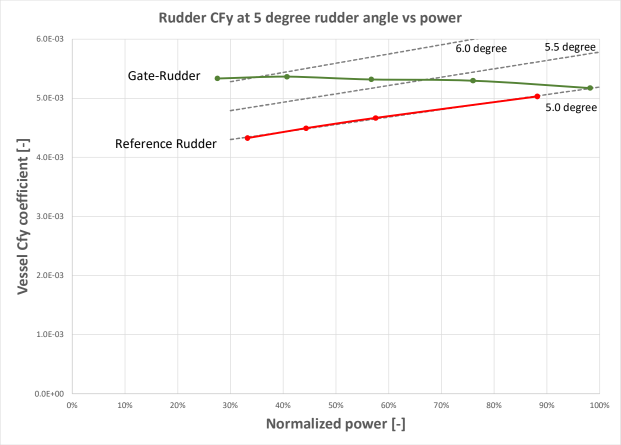

**Figure 14: Comparison of Sway-Force Coefficient at 5 degree Rudder Angle as Function of Propeller Power**

It should be kept in mind that the tight relation between propeller loading and vessel speed is valid for conventional propulsion, though it will be decoupled in case of WASP systems on deck. In case of favorable winds, the vessel will reach the target vessel speed with significantly lower propeller power. Still there will be a need for a certain amount of hull sway force to compensate the sway force from WASP equipment. The reduced effectiveness of a conventional rudder will then be compensated by increased rudder angles. This will come with additional rudder drag, based on the results as shown in Figure 13. Two dotted lines are drawn in Figure 14 to indicate the required additional rudder angle for different propeller loadings.

## 5 Dynamic system simulation modelling

All CFD simulations in the previous section covered a quasi-steady, non-equilibrium operating condition of the bulker vessel. To quickly find the actual equilibrium operating conditions, the available CFD data is transferred to a dynamic system simulation model. In line with the logic of the MMG modelling a 3DOF planar motion model is generated. With this dynamic model a large range of conditions can be evaluated quickly, since the simulations take a couple of seconds. This is very fast when compared to the run time of a single CFD condition which can be about a day for full convergence on a moderate cluster.

### 5.1 Dynamic System Model Main Blocks

The dynamic system simulation model is created in Simcenter Amesim, based on the planar motion model (3DOF). This model allows for the simulation of 2 forces and 1 moment, which would mean the surge and sway force and the yaw-moment. The actual vessel motions will include the effects of the inertia. The CFD results are used to determine the vessel response for the 3 components. In line with the MMG theory they are denoted with X for surge, Y for sway and N for yaw:

$$\begin{cases} X = X_H + X_{(P+R)} \\ Y = Y_{(H+P+R)} \\ N = N_{(H+P+R)} \end{cases} \tag{2}$$

It should be noted that the split of the different components differs. Whereas the MMG method splits into hull, propeller and rudder forces, here the overall vessel response is taken for the sway and yaw component. For the surge component the split is made between the resistance part (hull) and the thrust-producing part (propeller and rudder). For the reference rudder case, the impact of the rudder will also be combined with the propeller, albeit a negative contribution.

The forces and moment acting on the hull are made non-dimensional based on the vessel length (LPP) and draft d:

$$\begin{aligned} X'_H &= \frac{X_H}{\frac{1}{2}\rho \cdot LPP \cdot d \cdot v_{ship}^2} \\ Y' &= \frac{Y_{(H+P+R)}}{\frac{1}{2}\rho \cdot LPP \cdot d \cdot v_{ship}^2} \\ N' &= \frac{N_{(H+P+R)}}{\frac{1}{2}\rho \cdot LPP^2 \cdot d \cdot v_{ship}^2} \end{aligned} \tag{3}$$

The thrust producing parts (propeller and rudder) are scaled in line with known propeller scaling. Propeller torque is scaled in similar way:

$$\begin{aligned} Kt_{(P+R)} &= \frac{T}{\rho n^2 D^4} \\ Kq &= \frac{M}{\rho n^2 D^5} \end{aligned} \tag{4}$$

The multi-variable response-surface of the different components will be based on 4 parameters: dimensionless advance coefficient J, rudder steering angle δ, vessel drift velocity *v'* and turning rate *r'*, as shown in equation (5) for the Propeller and rudder surge force. The vessel drift velocity *v'* and the turning rate *r*' are made non-dimensionless in accordance with the MMG methodology.

$$Kt_{(P+R)} = f(J, \delta, v', r') \tag{5}$$

Once the actual vessel operating point has been found, the required propeller power is calculated. This is also based on a CFD-based response surface for Kq:

$$Kq = f(J, \delta, v', r') \tag{6}$$

Two types of response surfaces are defined: the even fit and the odd fit. A typical example for even fit would be the data as shown in Figure 13 and an odd fit for the data as shown in Figure 12.

The even fit is used for the hull surge force $X_h$ and the propeller characteristics $K_t$ and $K_q$. The formula for $K_t$ is given in equation 6, and a similar has been determined for $X_h$ and $K_q$.

$$\begin{aligned} Kt_{(P+R)} = {} & A + Bv' + Cv'^2 J + Dv'^4 + Ev'^2\delta^2 + \\ & + F\delta + G\delta^2 J + Hv'\delta^2 J + Ir' + Kr'^2 J + LJ \end{aligned} \tag{7}$$

The hull sway force and yaw moment are captured with the odd fit formula:

$$\begin{aligned} Y_{(H+P+R)} = {} & A + Bv' + Cv'J + Dv'^3 + \\ & + E\delta + F\delta J + Gr' + Hr'J \end{aligned} \tag{8}$$

The correlation between the CFD data and the response surface coefficients are plotted in the appendix for the 5 different data-sets.

To simulate the impact of WASP equipment, an additional external force can be applied to the model.

### 5.2 Control Loops in Dynamic Model

The underlying CFD data is based on constant vessel speed and variation of the propeller RPM. To test the dynamic model a control loop has been made to have a vessel speed control based on RPM. In this way the underlying CFD conditions can be checked easily and a fair comparison between different concepts can be made. In case the speed control is switched off, the simulations will be based on the input RPM of the propeller.

The second control loop is handling the course and heading control. In order to keep course, the rudder angle is adjusted. This ensures that the final destination of the vessel remains the same for different concepts.

### 5.3 Course-keeping with External Sway-Force

A rather simple example case is shown in Figures 15 and 16 where the vessel first ramps up the RPM to reach the target vessel speed. After certain time an external sway force is gradually introduced. This results in a response of the vessel with some drift angle and at the same time the control loops for the rudder start to work. The rudder angle is set to keep the straight-line course target in this simulation. Some subtle impact is observed on the propeller RPM as well to maintain the set target vessel speed.

The red line results represent the reference rudder and the green line the Gate-Rudder. In the chart for the ship speed it is difficult to see the red line, since the vessel speed controller manages to have both lines on top of each other. When looking at the propeller RPM a clear difference is seen. This slow running CPP is part of the overall concept to achieve good hydrodynamic efficiency. Comparison of the normalized power indicates a couple of percent lower shaft power for the Gate-Rudder concept. It should be noted that the mechanical losses from the gearbox and drive-line have not yet been included in this modelling.

When reviewing the vessel response on the external sway force both the vessel drift and the rudder angle act according to expectations. As mentioned before, the Gate-

Rudder is dimensioned to provide similar maneuvering characteristics as the reference rudder. This has been accomplished when looking at the small differences in applied rudder steering angles and achieved vessel drift angles. The small overshoot of both is a result of the course-keeping action after the ramp-up of the external force.

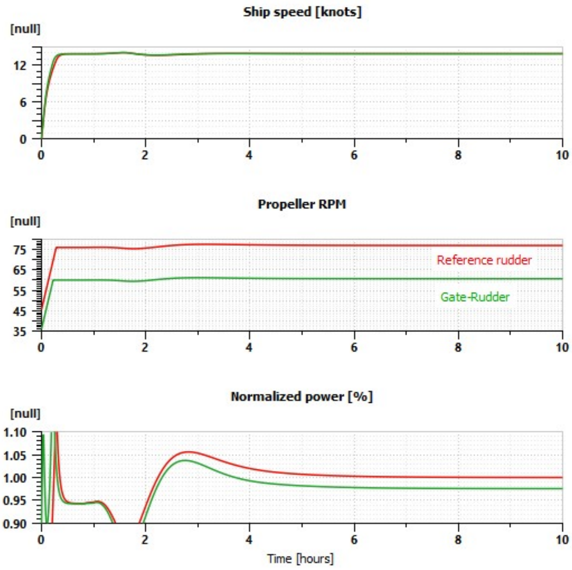

**Figure 15: Vessel Operation Output from Dynamic System Simulation**

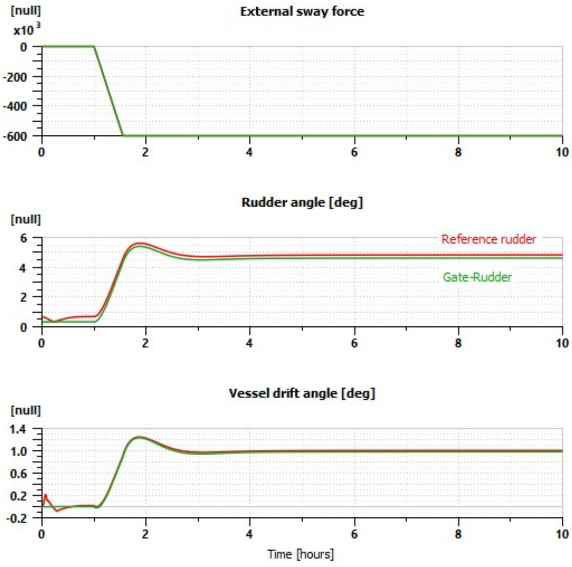

**Figure 16: Vessel and Rudder Response due to External Sway Force**

### 5.4 Coupling of System Simulation Results with CFD simulations

The dynamic model is based on a set of multi-parameter response-surfaces. To verify the accurate coupling between the underlying CFD data and the Amesim system simulation model a number of steps need to be taken.

First step is the transformation of the CFD data into the multi-variable response surfaces. Depending on the trends the underlying coefficients are either based on linear and 3rd order curves (for example sway force due to drift or steering) or based on quadratic curves (for example rudder drag due to steering). The aim is to capture all available trends of the data set, whilst keeping the order of the coefficients as low as possible. The quality of the different response surfaces is shown in the appendix, where $R^2$ correlation factors of 0.999 and higher have been achieved.

In the second step the table of coefficients from Excel is directly coupled with Amesim, to preserve all decimals as calculated in the response-surface methodology.

Third step is to check the modelling in Amesim and the validity of the coefficients. In this step the outcome from the dynamic simulation (propeller RPM, vessel speed, vessel drift angle, rudder angle) are used as input parameters for another CFD run. It has been proven that the calculated vessel forces are in equilibrium for surge direction. For the sway direction a net force equal to the prescribed initial sway force is found. Furthermore, the vessel yaw moment was negligible, indicating the stable course-keeping aspect.

## 6 MMG METHODOLOGY ADJUSTMENTS

The published MMG method by Yasukawa & Yoshimura (2015) is a valuable method to estimate the vessel maneuvering in the early phase. During the research of the Gate-Rudder concept some specific aspects of this twin-blade rudder system have been found. Even though it could be possible to tweak the MMG coefficients to get reasonable predictions, an alternative approach has been followed. The researchers of the MMG method decoupled the measured forces of the hull, propeller and rudder, based on theoretical models and known interaction effects. In the current approach, detailed data has been derived from full-scale CFD simulations. The CFD results allow for a detailed split of the forces acting on the different components, like the hull, propeller and rudder blades. To capture the behavior with a limited number of parameters (advance ratio J, rudder angle $\delta$, vessel drift velocity $v'$ and turning rate $r'$), it has been decided to take the responses, including their interaction effects in a lump-sum approach. The occurring interaction effects between the propeller and rudders as well as the interaction effects with the hull are part of the coefficient fitting at this moment. Consequently, it requires quite some simulation capacity to run all required CFD conditions to map the complete vessel behavior with sufficient accuracy. This can be regarded as a bottleneck at this moment in time, though this will improve over time, as observed with all CFD simulations last decades.

## 7 CONCLUSIONS AND OUTLOOK

As part of the CHEK EU-project an ’in silico’ study has been started on the performance of the Gate-Rudder concept for a bulker vessel. Given the interaction with Wind-Assisted-Ship-Propulsion (WASP) concepts, the effects of vessel drift and rudder steering angles have been included in the scope of work. Given the overall scope of CFD simulations with multiple variables and the comparison with a reference configuration, a number of simplifications in the numerical approach had to be applied. Work on further improving robustness and accuracy of the numerical results will be continued in the coming period.

Several phenomena as currently observed seem to be explainable with basic fluid dynamic principles and they are therefore worth mentioning:

- The Gate-Rudder concept with two blades allows for Toe-in/Toe-out angle adjustments in straight sailing. The forces on the two rudder blades are rather sensitive to small rudder angle variations. Toe-in rotation reduces the propeller loading slightly, which is of interest in case of fixed-pitch propeller applications.
- CFD simulations with vessel drift show a clear pre-rotation of the flow to the propeller. In hindsight this seems logic, though it impacts the propeller loading. This change of propeller loading can trigger interaction effects with the rudder blades and the aft part of the hull.
- Often Virtual Disks are used in CFD simulations, based on the axial inflow velocity. In case there is a pre-rotation due to vessel drift (or pre-swirl stators), then the validity of the Virtual Disk methodology might be compromised.
- The relationship between rudder sway force and drag is different for a Gate-Rudder compared to a conventional rudder. There are operating conditions where the Gate-Rudder blades give a positive contribution to the surge force, and in other conditions a significantly smaller drag contribution is found, whilst producing similar sway force.
- Reduction of propeller loading whilst maintaining a certain vessel speed is a typical (new) aspect of wind-assisted-propulsion. The effectiveness of the Gate-Rudder remains almost constant independent of the propeller loading, whereas conventional rudders in the slip-stream of the propeller will lose their effectiveness when the propeller loading reduces.
- Based on the presented data it seems that the benefits of Gate-Rudder occur in a so-called controlled 'disturbed flow' condition like drift angle or rudder steering angle. These conditions have so far in general been neglected in vessel performance assessments (like calm water straight sailing in towing tank).
- The known propeller-hull interaction effects (thrust-deduction, wake-fraction and relative rotative efficiency) are probably not sufficient to capture all effects of the Gate-Rudder concept accurately. Therefore, the system simulations approach based on the lump-sum data sets from CFD will be used for the moment.

Research of the Gate-Rudder concept will continue both based on numerical simulations (full-scale and model-scale) and model scale experiments. It will be essential to explore the effects of disturbed flows, next to the steady straight sailing conditions. This is partly related to the found benefits of sailing vessels with Gate-Rudder, which need to operate in the real-world dynamics and partly due to the CII regulations which will address real vessel operation with all its 'disturbances' like waves, wind, vessel motions and course-keeping and maneuvering aspects.

## 8 ACKNOWLEDGEMENTS

The work presented in this paper has been executed in EU-project CHEK, which has received funding from the European Union's Horizon 2020 research and innovation programme under grant agreement No 955286.

## REFERENCES

Aram, S., Mucha, P., 'Computational fluid dynamics analysis of different propeller models for a ship maneuvering in calm water', Ocean Engineering 276, 2023

Elger, D.E.,, Bentin, M., Vahs M., 'Comparison of different methods for predicting the drift angle and rudder resistance by wind propulsion systems on ships', Ocean Engineering, 217, 2020

Mizzi, K., Zammit Munro, M., Gurkan, A., Aktas, B., Atlar, M., Sasaki, N.,' The Performance Prediction and Energy Saving Evaluation for the Retrofit of a Gate Rudder System on a General Cargo Vessel using CFD ', 4th International Meeting - Ship Design & Optimization and Energy Efficient Devices for Fuel Economy', Istanbul, Turkey, 2022

Mucha, P., Aram, S., Radosavljevic, D., Pal Singh, J., Wheeler, M., 'Propeller Modeling for Ship Maneuvering Simulations in Simcenter STARCCM+', 25th Numerical Towing Tank Symposium (NuTTS), Ericeira, Portugal, 2023

Sasaki, N., Kuribayshi, S., Bulten, N, Yazawa, M., 'Joint sea trial of ships with Gate-Rudder and conventional rudder', Full Scale ship performance online conference, RINA, February 2021

Sasaki, N., Atlar, M., 'Design accuracy and errors of the Gate Rudder System of 'MW Erge" revealed by the GATERS project observations', Proceedings AMT'23 conference, Istanbul, Turkey, 2023

Yasukawa, H., Yoshimura, Y., 'Introduction of MMG standard method for ship maneuvering predictions', J. Mar Sci Technol (2015) 20:37-52

Zammit Munro, M., Mizzi, K., Gutteridge, K., Atlar, M., Sasaki, N., 'The Full-Scale Performance Prediction of a General Cargo Ship with a Retrofitted Gate Rudder System using CFD procedures', Proceedings OSES2023 conference, 2023

## APPENDIX

The concept of the multi-parameter response surface determination is explained briefly in this section and in the Figures below the correlation between the CFD data and the response surface coefficients are shown for the Gate-Rudder case.

The multi-parameter output is represented for example by:

$$Y_{(H+P+R)} = f(J, \delta, v', r') \tag{9}$$

The response surface is represented by equation 8, which means a least square fit for the 8 coefficients A till H. Based on the various CFD runs with different parameters for J, δ, $v'$and $r'$, the [A] matrix can be filled:

$$[A] \cdot [x] = \begin{bmatrix} 1 & v' & v'J & v'^3 & \delta & \delta J & r' & r'J \\ \vdots & \ddots & & & & & & \vdots \\ \vdots & & \ddots & & & & & \vdots \\ 1 & v' & v'J & v'^3 & \delta & \delta J & r' & r'J \end{bmatrix} \cdot \begin{bmatrix} A \\ B \\ C \\ D \\ E \\ F \\ G \\ H \end{bmatrix} = \begin{bmatrix} Y_1 \\ \vdots \\ \vdots \\ Y_n \end{bmatrix} \tag{10}$$

Solving this problem is rather simple with the following steps. First the A-matrix is multiplied by its transposed version to make it an [8x8] matrix:

$$[A]^T \cdot [A] \cdot [x] = [A]^T \cdot \begin{bmatrix} Y_1 \\ \vdots \\ \vdots \\ Y_n \end{bmatrix} \tag{11}$$

In the next step both sides are multiplied with the inverse of the [8x8] matrix:

$$\left[[A]^T \cdot [A]\right]^{-1} \cdot \left[[A]^T \cdot [A]\right] \cdot [x] = \left[[A]^T \cdot [A]\right]^{-1} \cdot [A]^T \cdot \begin{bmatrix} Y_1 \\ \vdots \\ \vdots \\ Y_n \end{bmatrix} \tag{12}$$

In this way the solution of the coefficients A till H is solved. The matrix operations can for example be executed in Excel:

$$\begin{bmatrix} A \\ B \\ C \\ D \\ E \\ F \\ G \\ H \end{bmatrix} = \left[[A]^T \cdot [A]\right]^{-1} \cdot [A]^T \cdot \begin{bmatrix} Y_1 \\ \vdots \\ \vdots \\ Y_n \end{bmatrix} \tag{13}$$

The methodology is based on the definition of equations 6 and 7. In case other combinations of parameters are required, the number of coefficients can be expanded. This will increase the number of column of the [A]-matrix, though it does not lead to problems in solving.

The outcome of the fitting process is shown in the Figures below for the different main components. As shown in the diagrams, the $R^2$ correlation is above 0.9996 for all.

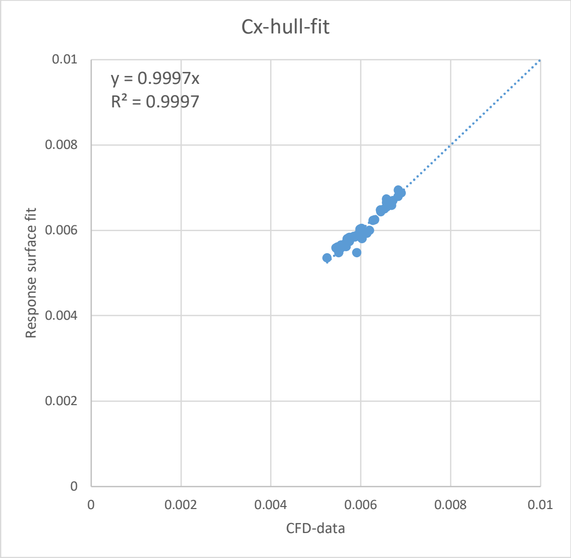

**Figure 17a: Cx-Hull Response Surface Correlation**

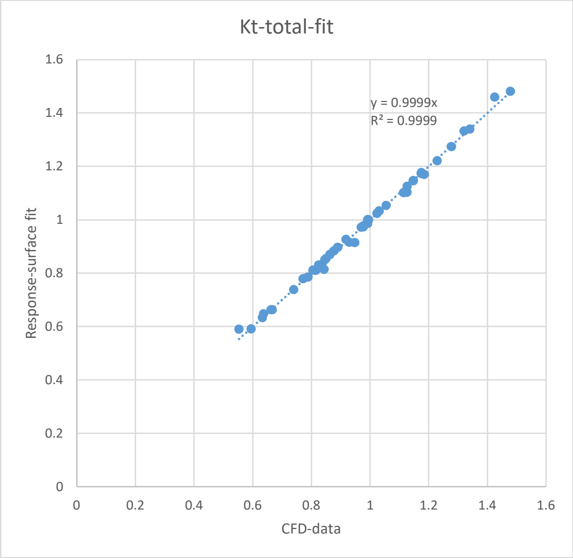

**Figure 17b: Kt-(prop+rudder) Response Surface Correlation**

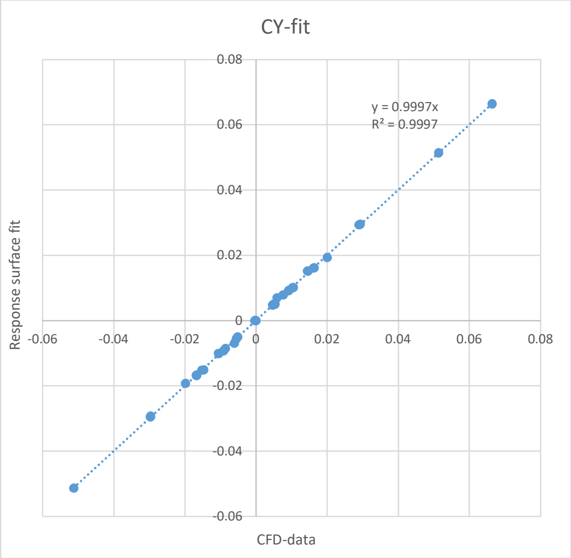

**Figure 17c: Cy-(hull-propeller-rudder) Response Surface Correlation**

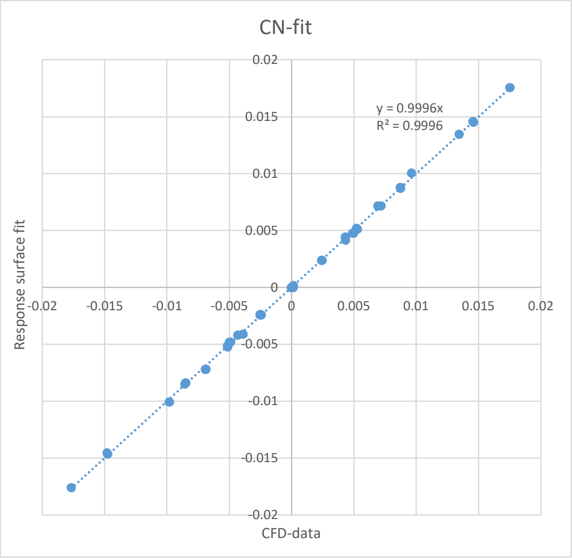

**Figure 17d: Cn-(hull-propeller-rudder) Response Surface Correlation**

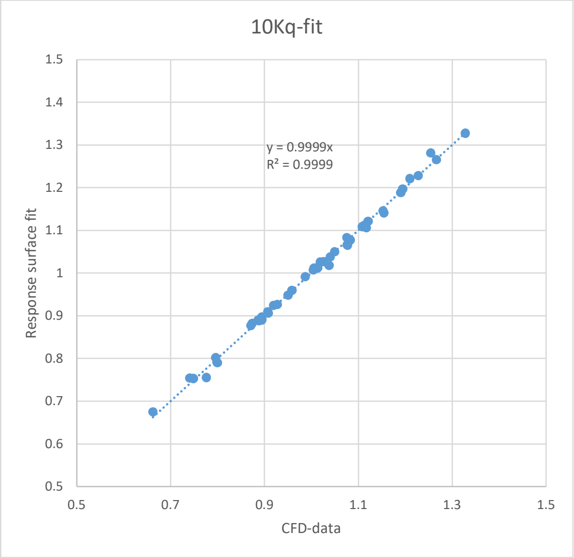

**Figure 17e: Kq-propeller Response Surface Correlation**